Transient kinetic analysis of oxidative dealkylation by the direct reversal DNA repair enzyme AlkB

Michael R. Baldwin, Suzanne J. Admiraal, Patrick J. O'Brien*

Department of Biological Chemistry, University of Michigan Medical School,
Ann Arbor, MI 48109-0600, USA.

*Corresponding author: Patrick O'Brien

E-mail: pjobrien@umich.edu

Running title: DNA repair kinetics of AlkB

Keywords: oxidative dealkylation, DNA repair, adaptive response, substrate specificity, *Escherichia coli*, AlkB, AlkA, AlkBH, pre-steady state kinetics, DNA adduct

Abstract

AlkB is a bacterial Fe(II)– and 2-oxoglutarate–dependent dioxygenase that repairs a wide range of alkylated nucleobases in DNA and RNA as part of the adaptive response to exogenous nucleic acid alkylating agents. Although there has been longstanding interest in the structure and specificity of *Escherichia coli* AlkB and its homologs, difficulties in assaying their repair activities have limited our understanding of their substrate specificities and kinetic mechanisms. Here, we used quantitative kinetic approaches to determine the transient kinetics of recognition and repair of alkylated DNA by AlkB. These experiments revealed that AlkB is a much faster alkylation repair enzyme than previously reported and that it is significantly faster than DNA repair glycosylases that recognize and excise some of the same base lesions. We observed that whereas 1,N^6-ethenoadenine can be repaired by AlkB with similar efficiencies in both single- and double-stranded DNA, 1-methyladenine is preferentially repaired in single-stranded DNA. Our results lay the groundwork for future studies of AlkB and its human homologs ALKBH2 and ALKBH3.

Introduction

DNA bases that are damaged by alkylation may cause mutations that lead to cell death or disease. Pathways for repair of alkylated bases in many organisms include base excision repair (BER) and direct reversal repair (DRR). For example, the adaptive response to alkylation damage in *Escherichia coli* includes both AlkA, a DNA glycosylase that initiates BER by excising alkylated bases, and AlkB, an oxidative dealkylase that uses ferrous iron, oxygen, and 2-oxoglutarate (2OG) to catalyze DRR of alkylated bases (1).

A broad range of alkylated nucleobases can be repaired by AlkB, including the monoalkyl substrate 1-methyladenine (1mA) and the exocyclic bridged substrate 1,N^6-ethenoadenine (εA) (2). AlkB-catalyzed hydroxylation of these alkyl adducts is followed by spontaneous release of an aldehyde byproduct to restore an undamaged nucleobase (Figure 1). Although a large number of AlkB substrates are known, information about its substrate specificity is limited. Previous studies of AlkB repair have often been qualitative or semi-quantitative in scope. The more quantitative studies among them have surveyed alkylated bases within dissimilar nucleic acid contexts using a wide variety of reaction conditions and assays, and these experimental differences have hindered efforts to combine results across studies into an accurate understanding of AlkB's substrate preferences. The tendency of members of the Fe(II)– and 2OG–dependent dioxygenase superfamily, which includes AlkB, to lose activity due to self-catalyzed oxidative modification further complicates interpretation of previous results (3-5).

In order to systematically study the substrate specificity and kinetic mechanism of AlkB, we developed a quantitative DNA glycosylase-coupled assay and used it to perform transient kinetic studies. This approach takes advantage of rapid reaction methods and single turnover reaction conditions to avoid the problem of dioxygenase inactivation during multiple turnover. The known AlkB substrates 1mA (6,7) and εA (8), embedded in both single-stranded (ss) and double-stranded (ds) DNA oligonucleotides of identical length and sequence, were chosen for direct comparison. Selection of 1mA was guided by the knowledge that *E. coli alkB* mutants are defective in processing methylated ssDNA (9), and 1mA forms appreciably in ssDNA exposed to alkylating agents (10). The εA oligonucleotides were included in the analysis because AlkB has been shown to be important for repair of a plasmid containing εA damage in *E. coli* cells (11). In addition, several well-characterized DNA glycosylases excise εA from dsDNA (12,13), so evaluation of oxidative dealkylation of the same lesion by AlkB allows recognition and repair of a common substrate by enzymes in the BER and DRR pathways to be compared.

Results

Metal binding to purified AlkB

Recombinant *E. coli* AlkB was purified without metal and stored in 1 mM EDTA to ensure protein stability. To evaluate the quality of the purified enzyme, we compared the total concentration of AlkB, as determined by its absorbance at 280 nm and its predicted extinction coefficient, to the total

concentration of metal that it binds, using ICP-MS to perform quantitative metal analysis. Fe^{2+} binds stoichiometrically in the AlkB active site and is required for oxidative repair of DNA by AlkB, but it is easily oxidized and can cause oxidative damage to AlkB in aerobic conditions. In the absence of Fe^{2+} the metal binding site of AlkB is able to bind to other metals, including Zn^{2+} (14-16). We performed parallel dialysis on AlkB samples that contained an excess of Zn^{2+} and on AlkB samples without added metal. At equilibrium each sample type is expected to contain the same amount of Zn^{2+}, corresponding to the concentration of AlkB that is capable of binding a metal ion in its active site. The molar ratio of zinc to AlkB was 0.92 ± 0.02 for extensively dialyzed samples that started with AlkB and an excess of Zn^{2+}, and 0.86 ± 0.06 for samples that started with AlkB only (Table S1). This result indicates that approximately 90% of the purified AlkB is competent to bind metal and is therefore expected to be enzymatically active.

DNA glycosylase-coupled assay for direct DNA repair catalyzed by AlkB

Some organisms that lack an AlkB homolog have DNA glycosylases with expanded substrate repertoires that are able to initiate base excision repair of known AlkB substrates (17-20), and we expected that such glycosylases would be useful for assaying AlkB and its homologs. The alkyladenine DNA glycosylase from *Bacillus subtilis* (bAAG; (21)) excises both the monoalkyl lesion 1mA and the exocyclic bridged lesion εA from DNA (Figure S1); we therefore developed a DNA glycosylase-coupled assay for AlkB using bAAG (Figure 2A). After AlkB repair reactions of fluorescein-labeled oligonucleotide substrates (Table S2) are quenched, bAAG is added to excise any unrepaired base lesions. The resultant abasic sites are cleaved by heating in sodium hydroxide, generating shortened strands that resolve from full-length AlkB-repaired products on a denaturing polyacrylamide gel (Figure 2B). The DNA glycosylase-coupled assay is suitable for any AlkB substrate for which there is a compatible glycosylase, and a similar assay that used *E. coli* MUG and human AAG has been applied to ethenobase-containing DNA (22).

Single turnover reactions of AlkB

Loss of catalytic activity for 2OG oxygenases is commonly observed and has been attributed to nonproductive reactions with oxygen, including auto-oxidation of active site residues and oxidation of the active site ferrous iron to a higher oxidation state (3-5). To avoid this problem, we initially applied the repair assay to single turnover reactions of AlkB. A single turnover requires less time than multiple turnovers, and the DNA concentration remains below the AlkB concentration in single turnover reactions ([AlkB] > [DNA]), minimizing time-dependent and potential DNA-dependent enzyme inactivation.

AlkB was purified without iron to ensure protein stability, therefore single turnover repair reactions required addition of the iron cofactor as well as the 2OG and DNA substrates. We compared two different orders of addition to assess whether or not the timing of DNA substrate addition mattered (Figure 3A). Representative timecourses for repair of εA-25mer (ssDNA) by an excess of AlkB are shown in Figure 3B and provide examples of the quality of kinetic data that can be obtained from the DNA glycosylase-coupled assay. Repair of εA-25mer is noticeably faster at all concentrations of AlkB (Figure 3C) when AlkB is combined with iron and 2OG *before* DNA substrate is added (OA2). Repair of εA•T-25mer (dsDNA), 1mA-25mer (ssDNA), and 1mA•T-25mer (dsDNA) is likewise faster for OA2 than for OA1 at all concentrations of AlkB (Figure S2; Table S3). The inhibitory effect of adding DNA substrate, iron, and 2OG simultaneously to AlkB reactions may be caused by nonproductive binding of DNA substrate to apo AlkB (E^{apo}), and it suggests that assembly of the AlkB active site is ordered (Figure 3D).

We focused on the more favorable OA2 conditions for comparison of single turnover repair of the DNA substrates εA-25mer, εA•T-25mer, 1mA-25mer, and 1mA•T-25mer by AlkB. This is likely to be the biologically relevant pathway, considering the physiological concentrations of Fe^{2+} and 2OG and the relative rarity of alkylated bases. The k_{obs} values determined from repair timecourses for all four substrates show a hyperbolic dependence on AlkB concentration (Figure 4), and their k_{max}, $K_{1/2}$, and $k_{max}/K_{1/2}$ values are summarized in Table 1. Our results are consistent with the prevailing view that 1mA in ssDNA is a preferred substrate of AlkB

(Table S4), and our single turnover methodology enables us to report this preference accurately and quantitatively: comparison of the substrate specificity constants $k_{max}/K_{1/2}$ reveals that AlkB prefers 1mA in ssDNA over 1mA in dsDNA by 18-fold, over εA in ssDNA by 160-fold, and over εA in dsDNA by 110-fold. The $k_{max}/K_{1/2}$ values for εA-25mer and εA•T-25mer are within 2-fold of one another, indicating that DNA strand context is less important for repair of εA than for repair of 1mA by AlkB. The similar maximal repair rate constants of ~1 s^{-1} for the 1mA and εA lesions, irrespective of the DNA strand context (k_{max}, Table 1), show that repair of εA by AlkB is limited by recognition, not rate of repair.

Multiple turnover reactions of AlkB are poorly behaved

Despite concerns about possible confounding nonproductive reactions with oxygen (3-5), we next applied the repair assay to multiple turnover reactions of AlkB, to facilitate more direct comparisons to previously published data (Table S4). However, inspection of multiple turnover timecourses for repair of 1mA•T-25mer by AlkB revealed that the rate of product formation decreases rapidly (Figure 5A), instead of staying constant during the first 10% of substrate depletion as expected for a well-behaved enzymatic reaction. This drop-off in 1mA repair during multiple turnover can be clearly seen by plotting the different instantaneous v/[E] values (calculated from three consecutive timepoints; Figure 5B); a similar drop-off is observed for εA repair during multiple turnover (Figure S3). To find out if instability of AlkB in our reaction conditions could account for the repair slowdown, we preincubated the enzyme at 37 °C for 90 min in reaction buffer only, or in reaction buffer plus all other reaction components, prior to adding DNA substrate to initiate multiple turnover repair (Figure 5C). There is no difference between the trajectories of the original reaction (Figure 5C, filled circles) and the reactions in which AlkB was preincubated (Figure 5C, open symbols), indicating that AlkB is stable for at least 90 min in our reaction conditions in the absence of DNA substrate. It is thus the addition of DNA substrate that causes the catalytic activity of AlkB to decrease in a time-dependent manner.

Many non-heme iron enzymes are known to undergo autocatalyzed oxidative modifications (3-5), which are postulated to result from side reactions of their highly activated Fe(IV)-oxo intermediates (23). Indeed, AlkB has been reported to self-hydroxylate Trp 178 (24), and hydroxylation and carbonylation of Leu 118 have also been detected (25). Such modifications may occur more readily in the presence of DNA, due to conformational changes in the AlkB active site that occur upon binding of DNA, and inactivating modifications could explain the observed slowdown in AlkB's repair rate during multiple turnover (Figure 5, Figure S3).

Multiple turnover competition assays to determine relative k_{cat}/K_M values for AlkB

After finding conventional multiple turnover reactions of AlkB to be poorly behaved, we turned to an alternative multiple turnover method to measure substrate specificity. The relative preference of AlkB for dealkylation of 1mA and εA in dsDNA was measured by placing 1mA•T-25mer and εA•T-19mer substrates (Table S2) in direct competition in the same AlkB reaction mixture (Figure 6). Following DNA glycosylase treatment and hydrolysis in our assay, the cleaved 1mA substrate (12mer) and its AlkB-repaired product (25mer) and the cleaved εA substrate (9mer) and its AlkB-repaired product (19mer) are all different sizes and can be resolved on a gel.

Repair of 1mA outcompetes repair of εA when equal concentrations of 1mA- and εA-containing dsDNA substrates are present in the same AlkB reaction mixture (Figure 6B), corresponding to a relative k_{cat}/K_M value of 9.3 ± 0.9 for 1mA•T-25mer with respect to εA•T-19mer (see Experimental Procedures). A slight length preference was observed when we controlled for the effect of DNA length on AlkB activity by performing a competition assay between εA incorporated into 25mer and 19mer duplexes (Figure 6C), which revealed a relative k_{cat}/K_M value of 1.3 ± 0.1 for εA•T-25mer with respect to εA•T-19mer.

The ratio of the two relative k_{cat}/K_M values for the 25mers with respect to εA•T-19mer gives a relative

k_{cat}/K_M value of 7.2 ± 0.9 for 1mA•T-25mer with respect to εA•T-25mer; this is the same, within error, as the relative $k_{max}/K_{1/2}$ value of 6.0 ± 3.0 for 1mA•T-25mer with respect to εA•T-25mer (Table 1; the ratio of their $k_{max}/K_{1/2}$ values). Therefore, results from multiple turnover competition between two alkylated substrates and from single turnover repair reactions performed for each substrate individually are in agreement and reveal that AlkB favors 1mA lesions over εA lesions in dsDNA by a factor of seven. This consistency validates the use of the single turnover specificity constant $k_{max}/K_{1/2}$ to evaluate the substrate specificity of AlkB, as an alternative to multiple turnover measurements that are adversely affected by AlkB inactivation. Notably, single turnover studies of substrate specificity and mechanism are widely used for another class of DNA repair enzymes, the DNA glycosylases, for which enzyme inhibition by the abasic DNA product often limits the value of multiple turnover measurements (26).

Discussion

A wide variety of alkylated nucleobases have been shown to be substrates of AlkB (2), but a quantitative understanding of its substrate specificity has been impeded by differences in how studies have been performed. For example, different studies of AlkB have used variable reaction conditions, DNA substrates of various lengths and sequences, and an array of assays. Not surprisingly, this diversity of substrates, reaction conditions, and experimental approaches has given rise to highly variable results that are difficult to interpret, as illustrated by the disparate kinetic parameters that have been reported for εA and 1mA substrates of AlkB and assembled in Table S4.

To analyze AlkB's substrate specificity quantitatively, we systematically compared its repair of εA and 1mA. The two alkylated bases were embedded in oligonucleotides of identical length and sequence in both ssDNA and dsDNA and assessed as substrates for AlkB in the same reaction conditions, using the same DNA-glycosylase coupled assay. Several limitations associated with previous studies of AlkB were overcome by using rapid reaction methods and a defined order of addition to investigate single turnover reactions, in conjunction with competition assays to compare representative multiple turnover reactions.

1mA in ssDNA is a preferred substrate of AlkB

E. coli alkB mutants are defective in processing methylated ssDNA (9), and 1mA is widespread in ssDNA that has been treated with alkylating agents (10). Consistent with these observations, our single turnover repair comparisons revealed a substantial preference of AlkB for 1mA in ssDNA. AlkB's substrate specificity constant $k_{max}/K_{1/2}$ is 18-fold larger for 1mA in 25 nt ssDNA than for 1mA in the same dsDNA sequence (Table 1; 1mA-25mer vs. 1mA•T-25mer). In contrast, $k_{max}/K_{1/2}$ values for ss εA-25mer and ds εA•T-25mer are within 2-fold of each other, indicating that DNA strand context matters little for repair of εA by AlkB. This difference in the importance of strand context for the 1mA and εA substrates may be due to differences in their base pairing with T (Figure 7). Although methylation of N1 of A prevents Watson-Crick base pairing between 1mA and T, they instead form a Hoogsteen base pair (27,28). Thus, hydrogen-bonding interactions between 1mA and T must be broken before AlkB can flip 1mA into its active site in dsDNA, but not in ssDNA, which may factor into AlkB's preference for 1mA in ssDNA. There are no hydrogen-bonding interactions between εA and T in dsDNA, so the energetic barrier for flipping εA into AlkB's active site is expected to be less dependent on strand context; this may account for the similar $k_{max}/K_{1/2}$ values for repair of ss εA-25mer and ds εA•T-25mer by AlkB. The $k_{max}/K_{1/2}$ ratios in Table 1 also reveal that although AlkB discriminates between 1mA and εA in ssDNA by a factor of 160, it has only a modest preference (6.0 ± 3.0) for 1mA over εA when both lesions are present in dsDNA. Importantly, multiple turnover competition reactions confirmed the modest preference (7.2 ± 0.9) for 1mA•T-25mer over εA•T-25mer.

Although the specificity of AlkB for each of the four substrates differs as described above, its maximal rate constants for their repair are all very similar (k_{max} values between 0.75 and 1.7 s^{-1}, Table 1). This high reactivity may come into play when AlkB is induced in *E. coli* as part of the adaptive response to alkylation damage (1): high AlkB

concentrations promote single turnover repair of lesions like εA, despite the weak specificity of AlkB for them. Consistent with this idea, AlkB was shown to play a major role in repair of a plasmid containing εA damage that had been introduced into *E. coli* cells, with increased repair detected in cells in which the adaptive response was induced (11).

Single turnover repair measurements reveal fast oxidative dealkylation by AlkB

Our single turnover repair measurements show that AlkB is a much faster oxidative dealkylase than has been appreciated. Previously reported or estimated k_{cat} values for repair of 1mA and εA in ssDNA by AlkB differ over wide ranges, from 0.007–0.2 s^{-1} for 1mA and from 0.001–0.03 s^{-1} for εA (Table S4). We used rapid reaction methods to measure the k_{max} value of 0.90 s^{-1} for repair of 1mA in ssDNA, which exceeds reported k_{cat} values by 5–100-fold (Table 1, Table S4). Likewise, the k_{max} value of 0.75 s^{-1} for repair of εA in ssDNA is 30–800-fold larger than reported k_{cat} values (Table 1, Table S4).

It is likely that loss of activity of AlkB over time and AlkB inhibition due to the order of addition of reaction components may have contributed to both the variability and the apparent underestimation of previous maximal rate measurements. We observed a rapid loss of AlkB activity during multiple turnover repair that prevented us from measuring steady state kinetic parameters for repair of 1mA and εA (Figure 5, Figure S3). Inactivating modifications of AlkB may be responsible for the observed slowdown in repair rate, because autocatalyzed oxidative modifications are well-known for Fe(II)/2OG-dependent dioxygenases (3-5) and oxidized AlkB variants have been found (24,25). Variable kinetic parameters such as those that have been reported for εA and 1mA substrates of AlkB (Table S4) are typical for enzymes that lose activity during reactions, because rarely shown experimental details such as the number and spacing of reaction timepoints and the timescales of reactions can have large effects on measurements. For example, if only a single reaction timepoint is collected then enzyme inactivation cannot be detected. Another experimental concern is the order of addition of reaction components used in previous AlkB studies. We observed that multiple turnover reactions, like single turnover reactions, are inhibited by OA1, the simultaneous addition of DNA substrate, iron, and 2OG to AlkB (Figure 3, Figure S2). Insufficient experimental detail is provided to know the order of addition that was used in most of the studies in Table S4, but the inhibitory OA1 was described in at least one of them.

Comparison of repair of εA in dsDNA by DRR and BER enzymes

While 1mA in ssDNA is a preferred substrate, AlkB also repairs εA in dsDNA (Table 1). The DNA glycosylase AlkA from *E. coli* initiates repair of εA in dsDNA by excising it (12,13), allowing the repair strategies of the two enzymes for this shared substrate to be compared. AlkB and AlkA have almost identical overall repair efficiencies for εA in dsDNA, with $k_{max}/K_{1/2}$ values of 2.0×10^5 $M^{-1}s^{-1}$ for dealkylation by AlkB (Table 1) and 1.6×10^5 $M^{-1}s^{-1}$ for base excision by AlkA (29). However, to achieve this repair efficiency AlkB couples high reactivity (k_{max} = 1.7 s^{-1}) with weak recognition of εA•T-DNA ($K_{1/2}$ = 8400 nM), whereas AlkA has an almost 400-fold lower k_{max} value (0.0045 s^{-1}) but a much higher substrate affinity ($K_{1/2}$ = 29 nM).

Both AlkA and AlkB are induced in *E. coli* as part of the adaptive response to alkylation damage, but AlkB appears to be the most important for *in vivo* repair of εA damage under standard growth conditions (11). Given the chemical differences in the AlkA- and AlkB-initiated pathways, it may be that each pathway contributes under different conditions. Cytoplasmic pH and availability of oxygen are two critical factors governing the relative proficiency of DRR and BER. Although the catalytic efficiency of AlkA matches that of AlkB under optimal glycosylase conditions at pH 6.1 (29), above this pH value AlkA shows a log-linear decrease in glycosylase activity (30). AlkB requires oxygen as a substrate and therefore DRR is only available under aerobic growth conditions. It is interesting to speculate that the coexistence of two separate DNA repair pathways, AlkA-initiated BER and AlkB-initiated DRR, provides broader

coverage for repair of alkylated DNA over a wider range of physiological conditions.

An experimental foundation for future studies of AlkB and its human homologs

The rapid reaction methods and DNA-glycosylase coupled assay that we developed and used to systematically compare 1mA and εA substrates can be extended to additional substrates to assess AlkB's substrate specificity more broadly. These approaches can also be applied to AlkB homologs, including the human proteins ALKBH2 and ALKBH3, which catalyze oxidative dealkylation of damaged DNA (2,31). Such studies will help to resolve discrepancies in reported kinetic parameters for ALKBH2 and ALKBH3, like those compiled for AlkB in Table S4, that currently obscure their substrate specificities. The differences in substrate preference that are uncovered for different AlkB homologs and for their site-specific variants will help to identify the molecular basis for discrimination between substrates, allowing rules for substrate selection by oxidative dealkylases to be defined and used to predict their activity towards novel forms of alkylation damage. Our results show that single turnover repair, with its short timescales and low DNA concentrations, is well-suited for evaluating substrate specificity for this family of repair enzymes, which may be prone to inactivation during multiple turnover repair like their prototypical member AlkB.

Experimental Procedures

Purification of AlkB

A pET19-derived expression construct for *E. coli* AlkB (15) was transformed into BL21(DE3) *E. coli*, and protein was expressed and purified as previously described (20). Purified protein was concentrated to 650 μM as determined by the absorbance at 280 nm using the predicted extinction coefficient of 32430 $M^{-1}cm^{-1}$. AlkB was purified without iron and stored in 1 mM EDTA to ensure protein stability.

Dialysis and ICP-MS of AlkB

Dialysis and ICP-MS were performed to determine the concentration of purified recombinant AlkB that is competent for binding zinc, for comparison to the concentration that was determined by absorbance at 280 nm. The dialysis buffer contained 25 mM HEPES (pH 7.5), 150 mM NaCl, and 0.1 mM TCEP, and buffer in the reservoir (250 mL) was supplemented with 0.25 μM $ZnSO_4$. AlkB was prepared at 25 μM in dialysis buffer with or without 250 μM $ZnSO_4$. Dialysis was performed at 4 °C in a 10-well microdialysis chamber (Spectra/Por) with each well containing 50 μL of analyte solution. Three wells contained AlkB with $ZnSO_4$, three wells contained AlkB without supplemental metal, two wells contained dialysis buffer with 250 μM $ZnSO_4$, and two wells contained dialysis buffer only. The free Zn^{2+} concentration was estimated to be 0.43 μM, 60-fold less than the concentration of AlkB in the wells but a 14-fold molar excess over total protein in the system. Dialysis proceeded for two days to reach equilibrium. Protein concentration was remeasured by absorbance at 280 nm as described above. Samples were then diluted in 0.5% nitric acid, and the zinc concentration was determined against a standard curve using a Nexion 2000 ICP-MS (Perkin Elmer).

Synthesis and purification of oligonucleotides

DNA substrates were synthesized by Integrated DNA Technologies or the Keck facility at Yale and were purified using denaturing PAGE as previously described (32). Sequences are provided in Table S2. ssDNA concentrations were determined from the absorbance at 260 nm using calculated extinction coefficients. For oligonucleotides containing εA, the extinction coefficient was calculated for the same sequence with an A in place of εA and corrected by subtracting 9400 $M^{-1}cm^{-1}$ to account for the weaker absorbance of εA (33). For oligonucleotides containing 1mA, the extinction coefficient was calculated for the same sequence with A in place of 1mA. Duplexes were annealed with 1.5-fold unlabeled complement.

DNA glycosylase-coupled assay for direct repair by AlkB

Single turnover reactions contained 50 nM–6.4 μM AlkB and 10–50 nM of a fluorescein-labeled ss or ds 25mer DNA substrate (Table S2), and typical multiple turnover reactions contained 5 nM AlkB and 1.2–1.4 uM of the same DNA substrates.

Reactions were carried out at 37 °C in reaction mixtures containing 25 mM HEPES (pH 7.5), 100 mM NaCl, 0.1 mg/mL BSA, 1 mM TCEP, 2 mM sodium L-ascorbate, 1 mM 2OG, and 40 μM ammonium iron (II) sulfate.

Kinetic parameters reported in the paper are from reactions that were initiated by adding DNA substrate to AlkB reactions after iron and 2OG had already been added (OA2; Figure 3A). However, for comparison some reactions were carried out using an alternate order of addition in which DNA substrate, iron, and 2OG were all added to AlkB reactions at the same time (OA1; Figure 3A), and the results of this comparison for single turnover reactions are shown in Table S3, Figure 3, and Figure S2.

For the fastest reactions, dealkylation is complete within seconds, requiring a rapid and efficient quench to stop the reaction. EDTA alone did not immediately stop reactions of AlkB, but a combination of EDTA and concentrated sodium hydroxide effectively stopped even the fastest reactions (Figure S4). Therefore, repair reaction aliquots were typically quenched with an equal volume of a solution of 12 mM EDTA in 200 mM sodium hydroxide, and these quenched aliquots were subsequently neutralized to pH ~7.2 with 0.5 volumes of 400 mM HEPES free acid. *B. subtilis* AAG was added to the neutralized samples to give a ≥2-fold excess of glycosylase over the DNA present in the neutralized samples, and an excess of the complementary DNA strand was also added at this time to samples that contained ssDNA substrates. After overnight incubation at room temperature to allow bAAG to convert any unrepaired DNA into abasic DNA, sodium hydroxide was added to a final concentration of 225 mM and samples were heated at 70 °C for 12 min to convert abasic sites into single-strand breaks. This glycosylase treatment converts unrepaired 25mer DNA into 12mer DNA, but 25mers that have been repaired by AlkB remain intact and appear as slower migrating product bands on gels (22). Hydrolyzed samples were mixed with formamide/EDTA loading buffer and analyzed by denaturing PAGE on 15 or 20% (w/v) gels containing 6.6 M urea. Gels were scanned using a Typhoon imager (GE Healthcare), and emission was measured with a 525BP40 filter following excitation of the fluorescein label at 488 nm. Fluorescence intensities of gel bands were quantified using ImageQuant TL (GE Healthcare) and corrected for the amount of background signal. The data were converted to fraction product (P) and then fit by the single exponential shown in Equation 1. Mock DNA repair reactions were performed for each DNA substrate in the absence of AlkB as a positive control for the DNA glycosylase activity of bAAG and to reveal the maximum amount of repairable DNA in each initial sample (end pt), which was 95% for the εA-25mer-containing substrates and 70–80% for the more synthetically challenging 1mA-25mer-containing substrates (Figure S1; (19,34)).

$$\text{fraction P} = \text{end pt}(1-\exp(-k_{obs}t) + \text{zero pt} \qquad \text{(Eq. 1)}$$

The concentration dependence of the single turnover rate constant (k_{obs}) was fit by a hyperbolic dependence (Equation 2), where k_{max} is the maximal single turnover rate constant, E is AlkB, and $K_{1/2}$ is the concentration of AlkB at which k_{obs} is 50% of the k_{max} value.

$$k_{obs} = (k_{max}[E])/(K_{1/2} + [E]) \qquad \text{(Eq. 2)}$$

When reactions were too fast to be followed using timepoints taken by hand, rapid mixing experiments were performed in a KinTek RFQ-3 quench-flow apparatus. For OA2, one sample loop contained AlkB, iron, and 2OG, and the other contained DNA substrate (Figure 3A), all at twice the final reaction concentration. Both samples were in reaction buffer and the drive syringes contained the same solution. Loaded reactants were allowed to equilibrate for 90 s to reach 37 °C. Reactions were initiated by mixing of 45 μl of each sample and were quenched at desired times by mixing with 90 μl of 12 mM EDTA in 200 mM hydroxide. Quenched aliquots were then neutralized and analyzed using the DNA-glycosylase coupled assay as described above.

To ensure that enzyme activity was retained during the time required to set up and then carry out typical reactions, we performed preincubation controls for AlkB. For all single and multiple turnover AlkB studies the preparation time was less than 30 min and reactions proceeded for a maximum of 30 min, so a 90 min preincubation time was tested. We

compared otherwise identical multiple turnover reactions of 1mA•T-25mer using AlkB that had not been preincubated, AlkB that had been preincubated at 37 °C for 90 min in reaction buffer and salt only, and AlkB that had been preincubated at 37 °C for 90 min in all reaction components except DNA. The reaction progress curves were indistinguishable (Figure 5C), indicating that AlkB is stable for at least 90 min in our reaction conditions before DNA substrate is added.

Competition assays to determine relative k_{cat}/K_M values for AlkB

The relative specificity of AlkB for dsDNA substrates containing εA and 1mA was determined using competition assays, with the substrate εA•T-19mer used as a reference (Table S2). As above, reactions were carried out using OA2 at 37 °C in reaction mixtures containing 25 mM HEPES (pH 7.5), 100 mM NaCl, 0.1 mg/mL BSA, 1 mM TCEP, 2 mM sodium L-ascorbate, 1 mM 2OG, and 40 μM ammonium iron (II) sulfate. Reactions initially contained 5 nM AlkB, 200 nM εA•T-19mer, and 200 nM of either 1mA•T-25mer or εA•T-25mer, and dealkylation activity was followed up to a maximum of 10% repair of either substrate. Samples were quenched and analyzed using the DNA-glycosylase coupled assay described above. Initial velocities are proportional to relative k_{cat}/K_M values as described in Equation 3 (35).

$$V_{S1}/V_{S2} = ((k_{cat}/K_M)^{S1} \times [S1])/((k_{cat}/K_M)^{S2} \times [S2]) \quad \text{(Eq. 3)}$$

Data availability: All data are contained within the article and accompanying supporting information.

Acknowledgments: We thank Thomas Hollis for providing an expression construct for AlkB, and Erin Taylor for cloning, purifying, and performing initial kinetic studies on the DNA glycosylase AAG from *B. subtilis*.

Funding and additional information: Funding was provided by a grant from the National Science Foundation (MCB-1615586, to P.J.O.). Research reported in this article was supported by the National Cancer Institute of the National Institutes of Health under Award Number P30CA046592 by the use of Rogel Cancer Center Shared Resources.

Conflict of Interest: The authors declare that they have no conflicts of interest with the contents of this article.

References

1. Sedgwick, B., and Lindahl, T. (2002) Recent progress on the Ada response for inducible repair of DNA alkylation damage. *Oncogene* **21**, 8886-8894
2. Fedeles, B. I., Singh, V., Delaney, J. C., Li, D., and Essigmann, J. M. (2015) The AlkB family of Fe(II)/α-ketoglutarate-dependent dioxygenases: repairing nucleic acid alkylation damage and beyond. *J. Biol. Chem.* **290**, 20734-20742
3. Hausinger, R. P. (2004) Fe(II)/α-ketoglutarate-dependent hydroxylases and related enzymes. *Crit. Rev. Biochem. Mol. Biol.* **39**, 21-68
4. Mantri, M., Zhang, Z., McDonough, M. A., and Schofield, C. J. (2012) Autocatalysed oxidative modifications to 2-oxoglutarate dependent oxygenases. *FEBS J.* **279**, 1563-1575
5. Farquhar, E. R., Koehntop, K. D., Emerson, J. P., and Que, L., Jr. (2005) Post-translational self-hydroxylation: a probe for oxygen activation mechanisms in non-heme iron enzymes. *Biochem. Biophys. Res. Commun.* **338**, 230-239
6. Trewick, S. C., Henshaw, T. F., Hausinger, R. P., Lindahl, T., and Sedgwick, B. (2002) Oxidative demethylation by *Escherichia coli* AlkB directly reverts DNA base damage. *Nature* **419**, 174-178
7. Falnes, P. O., Johansen, R. F., and Seeberg, E. (2002) AlkB-mediated oxidative demethylation reverses DNA damage in *Escherichia coli*. *Nature* **419**, 178-182
8. Delaney, J. C., Smeester, L., Wong, C., Frick, L. E., Taghizadeh, K., Wishnok, J. S., Drennan, C. L., Samson, L. D., and Essigmann, J. M. (2005) AlkB reverses etheno DNA lesions caused by lipid oxidation in vitro and in vivo. *Nat. Struct. Mol. Biol.* **12**, 855-860
9. Dinglay, S., Trewick, S. C., Lindahl, T., and Sedgwick, B. (2000) Defective processing of methylated single-stranded DNA by *E. coli* AlkB mutants. *Genes Dev.* **14**, 2097-2105
10. Singer, B., and Grunberger, D. (1983) *Molecular Biology of Mutagens and Carcinogens*, Plenum Press, New York
11. Maciejewska, A. M., Sokolowska, B., Nowicki, A., and Kusmierek, J. T. (2011) The role of AlkB protein in repair of 1,N^6-ethenoadenine in *Escherichia coli* cells. *Mutagenesis* **26**, 401-406
12. Saparbaev, M., Kleibl, K., and Laval, J. (1995) *Escherichia coli*, *Saccharomyces cerevisiae*, rat and human 3-methyladenine DNA glycosylases repair 1,N^6-ethenoadenine when present in DNA. *Nucleic Acids Res.* **23**, 3750-3755
13. Gros, L., Ishchenko, A. A., and Saparbaev, M. (2003) Enzymology of repair of etheno-adducts. *Mutat. Res.* **531**, 219-229
14. Koivisto, P., Duncan, T., Lindahl, T., and Sedgwick, B. (2003) Minimal methylated substrate and extended substrate range of *Escherichia coli* AlkB protein, a 1-methyladenine-DNA dioxygenase. *J. Biol. Chem.* **278**, 44348-44354
15. Holland, P. J., and Hollis, T. (2010) Structural and mutational analysis of *Escherichia coli* AlkB provides insight into substrate specificity and DNA damage searching. *PLoS One* **5**, e8680

16. Ergel, B., Gill, M. L., Brown, L., Yu, B., Palmer, A. G., 3rd, and Hunt, J. F. (2014) Protein dynamics control the progression and efficiency of the catalytic reaction cycle of the *Escherichia coli* DNA-repair enzyme AlkB. *J. Biol. Chem.* **289**, 29584-29601
17. Leiros, I., Nabong, M. P., Grosvik, K., Ringvoll, J., Haugland, G. T., Uldal, L., Reite, K., Olsbu, I. K., Knaevelsrud, I., Moe, E., Andersen, O. A., Birkeland, N. K., Ruoff, P., Klungland, A., and Bjelland, S. (2007) Structural basis for enzymatic excision of N1-methyladenine and N3-methylcytosine from DNA. *EMBO J.* **26**, 2206-2217
18. Moe, E., Hall, D. R., Leiros, I., Monsen, V. T., Timmins, J., and McSweeney, S. (2012) Structure-function studies of an unusual 3-methyladenine DNA glycosylase II (AlkA) from *Deinococcus radiodurans*. *Acta. Crystallogr. D Biol. Crystallogr.* **68**, 703-712
19. Shi, R., Mullins, E. A., Shen, X. X., Lay, K. T., Yuen, P. K., David, S. S., Rokas, A., and Eichman, B. F. (2018) Selective base excision repair of DNA damage by the non-base-flipping DNA glycosylase AlkC. *EMBO J.* **37**, 63-74
20. Admiraal, S. J., Eyler, D. E., Baldwin, M. R., Brines, E. M., Lohans, C. T., Schofield, C. J., and O'Brien, P. J. (2019) Expansion of base excision repair compensates for a lack of DNA repair by oxidative dealkylation in budding yeast. *J. Biol. Chem.* **294**, 13629-13637
21. Aamodt, R. M., Falnes, P. O., Johansen, R. F., Seeberg, E., and Bjoras, M. (2004) The *Bacillus subtilis* counterpart of the mammalian 3-methyladenine DNA glycosylase has hypoxanthine and 1,N^6-ethenoadenine as preferred substrates. *J. Biol. Chem.* **279**, 13601-13606
22. Zdzalik, D., Domanska, A., Prorok, P., Kosicki, K., van den Born, E., Falnes, P. O., Rizzo, C. J., Guengerich, F. P., and Tudek, B. (2015) Differential repair of etheno-DNA adducts by bacterial and human AlkB proteins. *DNA Repair (Amst.)* **30**, 1-10
23. Krebs, C., Galonic Fujimori, D., Walsh, C. T., and Bollinger, J. M., Jr. (2007) Non-heme Fe(IV)-oxo intermediates. *Acc. Chem. Res.* **40**, 484-492
24. Henshaw, T. F., Feig, M., and Hausinger, R. P. (2004) Aberrant activity of the DNA repair enzyme AlkB. *J. Inorg. Biochem.* **98**, 856-861
25. Sundheim, O., Vagbo, C. B., Bjoras, M., Sousa, M. M., Talstad, V., Aas, P. A., Drablos, F., Krokan, H. E., Tainer, J. A., and Slupphaug, G. (2006) Human ABH3 structure and key residues for oxidative demethylation to reverse DNA/RNA damage. *EMBO J.* **25**, 3389-3397
26. Coey, C. T., and Drohat, A. C. (2017) Kinetic methods for studying DNA glycosylases functioning in base excision repair. *Methods Enzymol.* **592**, 357-376
27. Nikolova, E. N., Zhou, H., Gottardo, F. L., Alvey, H. S., Kimsey, I. J., and Al-Hashimi, H. M. (2013) A historical account of Hoogsteen base-pairs in duplex DNA. *Biopolymers* **99**, 955-968
28. Yang, C. G., Garcia, K., and He, C. (2009) Damage detection and base flipping in direct DNA alkylation repair. *ChemBioChem* **10**, 417-423
29. Taylor, E. L., and O'Brien, P. J. (2015) Kinetic mechanism for the flipping and excision of 1,N^6-Ethenoadenine by AlkA. *Biochemistry* **54**, 898-908
30. O'Brien, P. J., and Ellenberger, T. (2004) The *Escherichia coli* 3-methyladenine DNA glycosylase AlkA has a remarkably versatile active site. *J. Biol. Chem.* **278**, 26876-26884
31. Zheng, G., Fu, Y., and He, C. (2014) Nucleic acid oxidation in DNA damage repair and epigenetics. *Chem. Rev.* **114**, 4602-4620
32. Hedglin, M., and O'Brien, P. J. (2008) Human alkyladenine DNA glycosylase employs a processive search for DNA damage. *Biochemistry* **47**, 11434-11445
33. Secrist, J. A., 3rd, Barrio, J. R., Leonard, N. J., and Weber, G. (1972) Fluorescent modification of adenosine-containing coenzymes. Biological activities and spectroscopic properties. *Biochemistry* **11**, 3499-3506
34. Tang, Q., Cai, A., Bian, K., Chen, F., Delaney, J. C., Adusumalli, S., Bach, A. C., 2nd, Akhlaghi, F., Cho, B. P., and Li, D. (2017) Characterization of byproducts from chemical syntheses of oligonucleotides containing 1-methyladenine and 3-methylcytosine. *ACS Omega* **2**, 8205-8212
35. Fersht, A. (1999) *Structure and Mechanism in Protein Science*, W. H. Freeman and Company, New York

36. Mishina, Y., Yang, C. G., and He, C. (2005) Direct repair of the exocyclic DNA adduct 1,N^6-ethenoadenine by the DNA repair AlkB proteins. *J. Am. Chem. Soc.* **127**, 14594-14595
37. Roy, T. W., and Bhagwat, A. S. (2007) Kinetic studies of *Escherichia coli* AlkB using a new fluorescence-based assay for DNA demethylation. *Nucleic Acids Res.* **35**, e147
38. Ringvoll, J., Moen, M. N., Nordstrand, L. M., Meira, L. B., Pang, B., Bekkelund, A., Dedon, P. C., Bjelland, S., Samson, L. D., Falnes, P. O., and Klungland, A. (2008) AlkB homologue 2-mediated repair of ethenoadenine lesions in mammalian DNA. *Cancer Res.* **68**, 4142-4149
39. Yu, B., and Hunt, J. F. (2009) Enzymological and structural studies of the mechanism of promiscuous substrate recognition by the oxidative DNA repair enzyme AlkB. *Proc. Natl. Acad. Sci. U.S.A.* **106**, 14315-14320
40. Maciejewska, A. M., Poznanski, J., Kaczmarska, Z., Krowisz, B., Nieminuszczy, J., Polkowska-Nowakowska, A., Grzesiuk, E., and Kusmierek, J. T. (2013) AlkB dioxygenase preferentially repairs protonated substrates: specificity against exocyclic adducts and molecular mechanism of action. *J. Biol. Chem.* **288**, 432-441
41. Zhu, C., and Yi, C. (2014) Switching demethylation activities between AlkB family RNA/DNA demethylases through exchange of active-site residues. *Angew. Chem. Int. Ed. Engl.* **53**, 3659-3662
42. Chen, F., Tang, Q., Bian, K., Humulock, Z. T., Yang, X., Jost, M., Drennan, C. L., Essigmann, J. M., and Li, D. (2016) Adaptive response enzyme AlkB preferentially repairs 1-methylguanine and 3-methylthymine adducts in double-stranded DNA. *Chem. Res. Toxicol.* **29**, 687-693
43. Chen, F., Bian, K., Tang, Q., Fedeles, B. I., Singh, V., Humulock, Z. T., Essigmann, J. M., and Li, D. (2017) Oncometabolites D- and L-2-hydroxyglutarate inhibit the AlkB family DNA repair enzymes under physiological conditions. *Chem. Res. Toxicol.* **30**, 1102-1110

Footnotes

The abbreviations used are: BER, base excision repair; DRR, direct reversal repair; 2OG, 2-oxoglutarate; 1mA, 1-methyladenine; εA, 1,N^6-ethenoadenine; ss, single-stranded; ds, double-stranded; bAAG, alkyladenine DNA glycosylase from *B. subtilis;* OA1, order of addition in which DNA substrate, iron, and 2OG are added simultaneously to reaction mixtures containing AlkB; OA2, order of addition in which DNA substrate is added to reaction mixtures after AlkB, iron, and 2OG have already been combined; TCEP, tris(2-carboxyethyl)phosphine.

Table 1. Single-turnover rate constants for repair of alkylated adenine bases by AlkB.[a]

Substrate	k_{max} **(s^{-1})**	$K_{1/2}$ **(nM)**	$k_{max}/K_{1/2}$ **($M^{-1}s^{-1}$)**	$k_{max}/K_{1/2}$ **(relative)**
1mA-25mer	0.90 ± 0.03	41 ± 7	$(2.2 \pm 0.4) \times 10^7$	(1)
1mA•T-25mer	0.77 ± 0.02	650 ± 50	$(1.2 \pm 0.1) \times 10^6$	0.055
εA-25mer	0.75 ± 0.11	5300 ± 1300	$(1.4 \pm 0.4) \times 10^5$	0.0064
εA•T-25mer	1.7 ± 0.5	8400 ± 3400	$(2.0 \pm 1.0) \times 10^5$	0.0091

[a] At 37 °C and pH 7.5 (25 mM HEPES, 100 mM NaCl, 1 mM TCEP, 0.1 mg/mL BSA, 1 mM 2OG, 40 μM ammonium iron (II) sulfate, and 2 mM sodium L-ascorbate). DNA substrate was added to reaction mixtures after AlkB, iron, and 2OG had already been combined (OA2; Figure 3A).

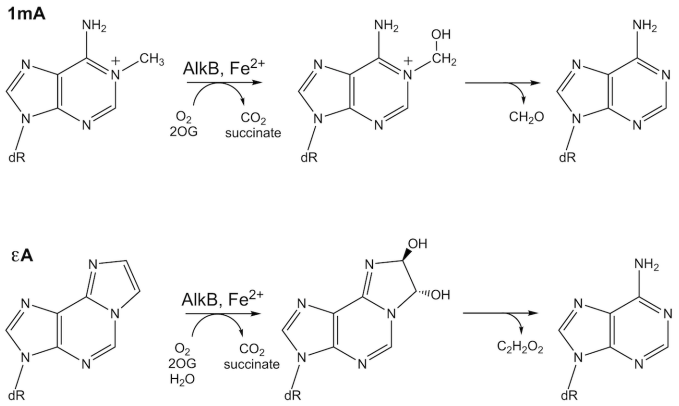

Figure 1. Repair of 1mA, a monoalkyl substrate, and εA, an exocyclic bridged substrate, in DNA by AlkB-catalyzed oxidative dealkylation.

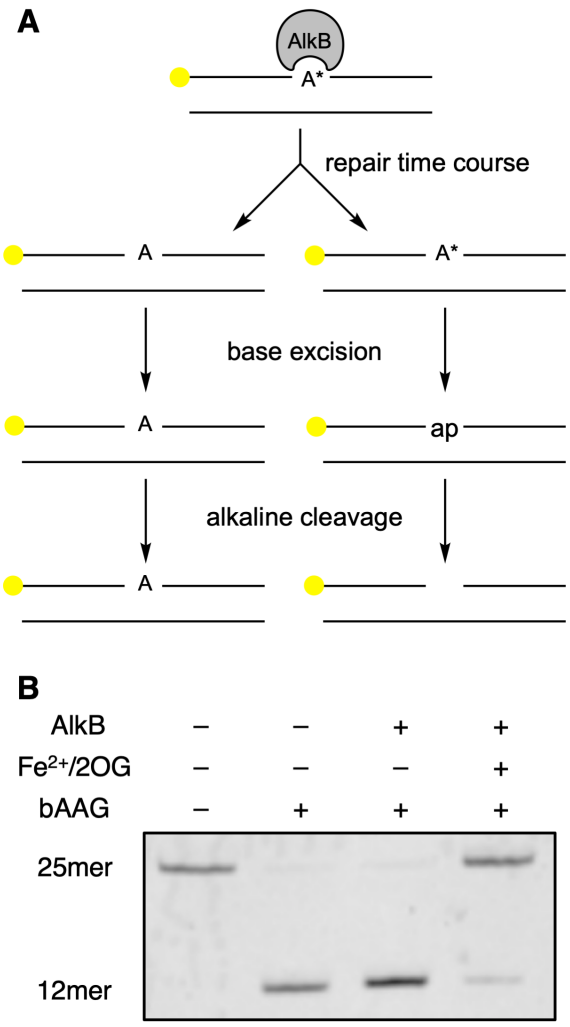

Figure 2. DNA glycosylase-coupled assay for alkylation repair. (A) A fluorescein-labeled oligonucleotide substrate containing an alkylated base lesion (A*) is incubated with AlkB and cosubstrates. The repair reaction is quenched with EDTA and sodium hydroxide and then neutralized. Unrepaired base lesions (right pathway) are excised by a DNA glycosylase, yielding abasic sites (ap) that are cleaved when heated in sodium hydroxide to generate shortened strands that resolve from the stable repaired product (left pathway) on a denaturing polyacrylamide gel. For repair reactions of ssDNA substrates, an excess of the complementary strand was included in the quench solution to improve subsequent DNA glycosylase activity. (B) A gel image shows the mobility of species present after εA-25mer is incubated with the indicated components. After a complete dealkylation reaction (far right lane), nearly all of the εA base has been converted to A, which is not excised by bAAG, resulting in a repaired product that runs as an intact 25mer.

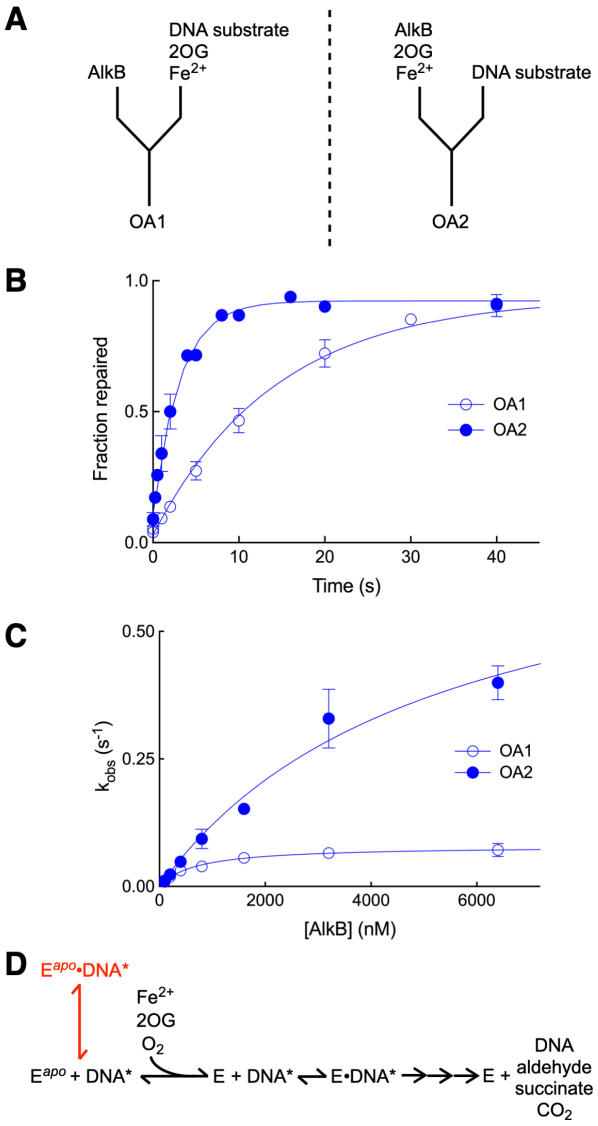

Figure 3. The order of addition of reaction components affects single turnover repair kinetics of AlkB. (A) Schematic of the two orders of addition, OA1 and OA2, that were compared for AlkB repair reactions. (B) Timecourses for repair of 25 nM εA-25mer by 3.2 μM AlkB, measured using OA1 (open circles) and OA2 (filled circles). Each reaction progress curve was fit by a single exponential, giving observed rate constants (k_{obs}) of 0.069 s^{-1} for OA1 and 0.32 s^{-1} for OA2. (C) The dependence of single turnover repair rate constants for εA-25mer on the AlkB concentration differs for OA1 (open circles) and OA2 (closed circles) but is hyperbolic for both orders of addition, and k_{max} and $K_{1/2}$ values for repair are reported in Table S2. The average of 2–4 reactions is shown ± SD. (D) Model for nonproductive binding of alkylated DNA substrate (DNA*) to *apo* AlkB (E^{apo}) that may account for the inhibitory effect of OA1 on repair reactions.

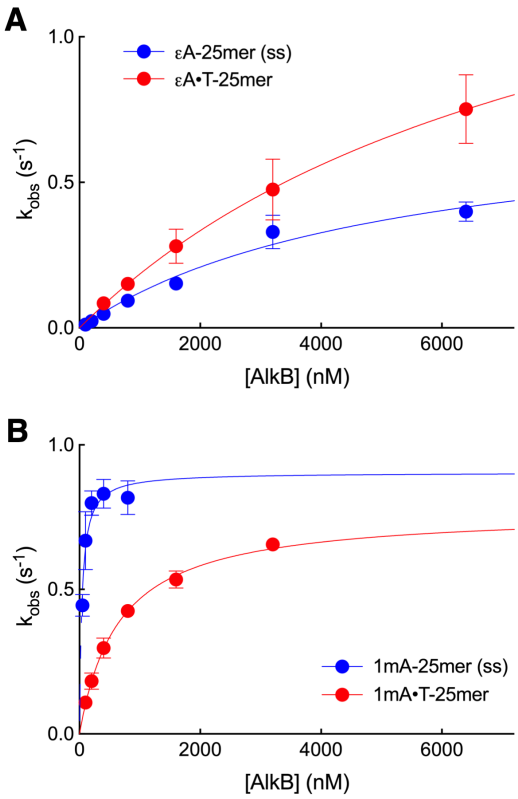

Figure 4. AlkB-catalyzed single turnover repair of εA and 1mA in ssDNA and dsDNA. (A) Dependence of single turnover repair rate constants for εA-25mer and εA•T-25mer on the AlkB concentration. (B) Dependence of single turnover repair rate constants for 1mA-25mer and 1mA•T-25mer on the AlkB concentration. The single turnover repair rate constants for each substrate exhibited a hyperbolic dependence on AlkB concentration, and k_{max} and $K_{1/2}$ values for repair of the four substrates are reported in Table 1. OA2 conditions were used, and the average of 2–4 reactions is shown ± SD.

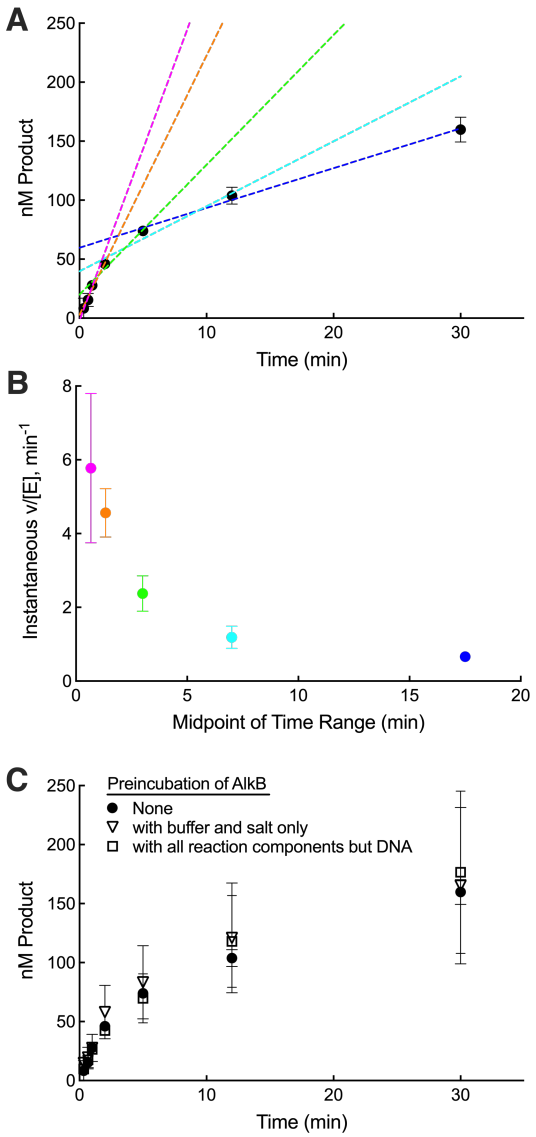

Figure 5. The rate of multiple turnover repair of 1mA•T-25mer by AlkB decreases over time. (A) Timecourse for repair of 1.2 µM 1mA•T-25mer by 5 nM AlkB. The dashed lines show the decreasing instantaneous rates of repair (v) calculated from linear fits of each three consecutive timepoints. (B) The decreasing v/[E] for repair of 1.2 µM 1mA•T-25mer by AlkB, with symbols colored to match the corresponding dashed lines in A. (C) Timecourses for repair of 1.2 µM 1mA•T-25mer by 5 nM AlkB, with or without preincubation of AlkB at 37 °C for 90 min with reaction components prior to adding DNA substrate to initiate multiple turnover repair. The average of 2–4 reactions is shown ± SD.

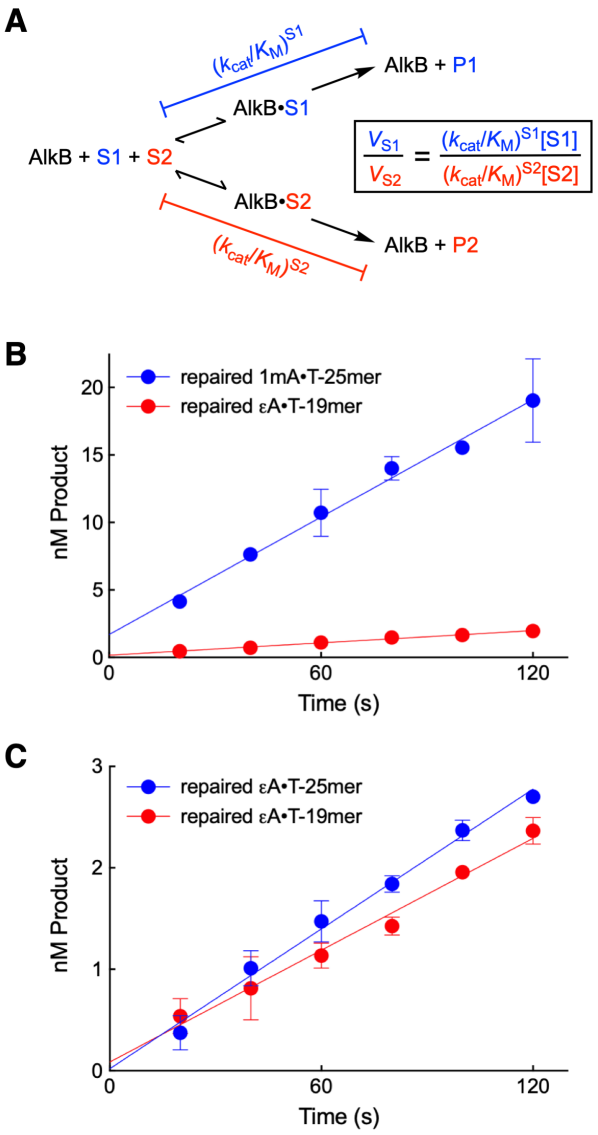

Figure 6. Steady-state competition experiments for AlkB-catalyzed oxidative dealkylation. (A) Schematic for a direct competition experiment. The relative k_{cat}/K_M value for two competing substrates (S1, S2) present in the same AlkB reaction mixture can be determined from the initial rates (V) and the initial substrate concentrations. (B) A relative k_{cat}/K_M value of 9.3 ± 0.9 was determined for 1mA•T-25mer with respect to the reference substrate εA•T-19mer. (C) A relative k_{cat}/K_M value of 1.3 ± 0.1 was determined for εA•T-25mer with respect to εA•T-19mer, indicating a slight length preference for the 25mer. Reactions contained 5 nM AlkB and 200 nM of each dsDNA. The average of two reactions is shown ± SD.

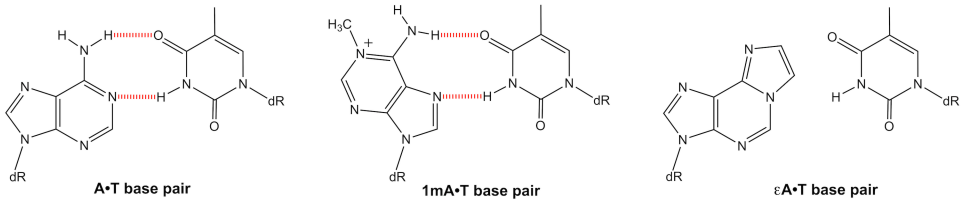

Figure 7. Base pairing of A, 1mA, and εA with T. Hydrogen-bonding interactions in the Watson-Crick base pair favored by A•T and the Hoogsteen base pair favored by 1mA•T are shown in red. Methylation of A prevents Watson-Crick base pairing between 1mA and T, and the damaged 1mA base instead flips to adopt a *syn* conformation within a Hoogsteen base pair. The εA base cannot hydrogen bond with T.